

Neutron scattering studies and modeling of high mobility group 14 core nucleosome complex

(chromatin/gene activation/transcription)

EDWARD C. UBERBACHER*, JAMES K. W. MARDIAN*†, RANDALL M. ROSSI*, DONALD E. OLINS*, AND GERARD J. BUNICK*‡§

*University of Tennessee–Oak Ridge Graduate School of Biomedical Sciences and Biology Division; and ‡Chemistry Division, Oak Ridge National Laboratory, Oak Ridge, Tennessee 37830

Communicated by Peter H. von Hippel, May 13, 1982

ABSTRACT Considerable evidence relates the nonhistone proteins high mobility group (HMG) 14 and HMG 17 with the structure of active or potentially active chromatin. In this study, bulk nucleosome core particles prepared from chicken erythrocytes and the complex formed by binding two HMG 14 molecules per nucleosome core were studied by use of small-angle neutron scattering techniques. By varying the $H_2O/{}^2H_2O$ ratio, and hence the contrast between the solvent and the particles, it was possible to determine the radius of gyration of the protein and of the DNA independently and as a function of HMG 14 binding. The results show an increase of $0.9 \pm 0.6 \text{ \AA}$ (mean \pm SEM) in the protein radius of gyration and of $2.7 \pm 0.6 \text{ \AA}$ in the DNA radius of gyration upon binding of HMG 14 to the nucleosome. These changes are considered in the light of several postulated modes for the unfolding or perturbation of the nucleosome structure. Modeling calculations demonstrate that the observed changes in radius of gyration for the DNA and for the protein are too small to be consistent with an overall unfolding or opening of the core particle upon HMG 14 binding. However, the observed changes are consistent with several models that involve only minor changes in the structure. It is postulated that the differences observed may be an indication of the type of conformational change occurring in active nucleosomes.

The nucleosome is universally accepted as constituting the first level of DNA organization in eukaryotic organisms (1, 2). Although the general structure of the nucleosome core particle is fairly well established (3–6), little is known about the dynamics of the structure and the interaction of potential effector proteins such as ubiquitin or the high mobility group (HMG) non-histone chromosomal proteins.

HMG 14 and HMG 17 are categorized as structural proteins that are associated with potentially active regions of chromatin (7). Studies have shown that mononucleosomes preferentially released from chromatin by micrococcal nuclease digestion contain HMG 14 and HMG 17 and are also enriched in expressed DNA sequences (7, 8). Reconstitution studies provide further evidence that active or potentially active regions of chromatin, as identified by DNase I sensitivity, are associated with the HMG 14 and HMG 17 (9, 10).

The interaction of isolated nucleosome core particles with purified HMG 14 or HMG 17 under appropriate conditions results in the formation of a complex containing two HMG 14 or HMG 17 molecules per nucleosome (11). The binding affinity is high, and the binding sites appear to be the same for HMG 14 and HMG 17. Under appropriate ionic conditions, the HMG binding is cooperative (8). The binding of HMG 14 to nucleosome core particles reconstituted from inner histones and

poly(dA-dT) alters the frequency distribution of nucleolytic action by DNase I without significantly changing the overall rate of nucleolysis (11). The manner in which the frequency distribution of DNA fragments changes indicates that the bound HMG 14 (or HMG 17) molecules protect one section of the DNA superhelix 5–25 base pairs from each end from nucleolysis and another section of the DNA superhelix 35–55 base pairs from each end becomes more accessible to the DNase I and thus shows enhanced nucleolysis (11).

Here we report the effect of HMG 14 binding to bulk nucleosome core particles as studied by comparison of neutron-scattering curves collected for the core particle and the nucleosome–HMG 14 complex at several $H_2O/{}^2H_2O$ ratios. By using appropriate mixtures of H_2O and 2H_2O , the mean scattering length density can be adjusted over a range encompassing the mean scattering length density of the nucleosomal protein core (protein match point; scattering from DNA predominates) and the mean scattering length density of DNA (DNA match point; scattering from protein core predominates). Contrast variation enables determination of the effects of HMG binding on the conformation of both the nucleosomal protein core and the DNA superhelix.

MATERIALS AND METHODS

Nucleosomes. Nucleosome core particles were isolated from chicken erythrocyte nuclei by a modified version of the procedure described by Lutter (12). Nucleosome core particles isolated according to this procedure contain 146 nucleotide pairs of DNA and a full complement of intact core histones.

HMG 14. Chicken erythrocyte nuclei were prepared from 35 liters of chicken blood, washed once in 155 liters of RSB (10 mM NaCl/10 mM Tris, pH 7.4/3 mM $MgCl_2$), resuspended in 190 liters of RSBN (10 mM NaCl/10 mM Tris, pH 7.4/3 mM $MgCl_2$ /0.05% Nonidet P-40), and pelleted. The pellet was then treated with 0.35 M NaCl and precipitated with 2% trichloroacetic acid, as described by Goodwin (13), to remove low mobility group (LMG) proteins. The HMG proteins were recovered from the supernatant by acetone precipitation. Fractionation of HMG 14 and HMG 17 was performed strictly according to the method described by Rabbani (14). Purified HMG proteins were lyophilized and then stored at $-20^\circ C$.

Neutron Scattering Procedure. Neutron scattering measurements were made on the 30-m small-angle neutron scattering (SANS) instrument of the National Center for Small-Angle Scattering Research located at the High Flux Isotope

The publication costs of this article were defrayed in part by page charge payment. This article must therefore be hereby marked "advertisement" in accordance with 18 U. S. C. §1734 solely to indicate this fact.

Abbreviations: HMG, high mobility group; LMG, low mobility group.
† Present address: Garrett Turbine Engine Company, P. O. Box 5217, Phoenix, AZ 85010.

§ To whom reprint requests should be addressed.

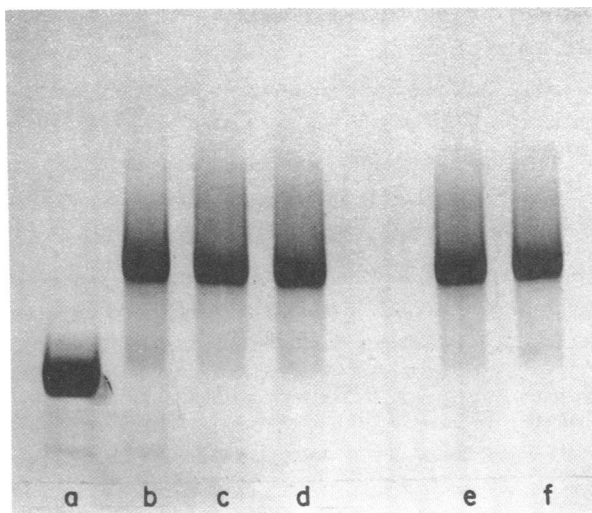


FIG. 1. Particle gel showing formation of the nucleosome-HMG 14 complex. Lanes: a, mononucleosome standard; b, nucleosome-HMG 14 complex from $^2\text{H}_2\text{O}$ sample; c, from 75% $^2\text{H}_2\text{O}$ sample; d, from 50% $^2\text{H}_2\text{O}$ sample; e, from 25% $^2\text{H}_2\text{O}$ sample; f, from H_2O sample. Particle gel was run in $0.3\times$ TBE in H_2O .

Reactor at Oak Ridge National Laboratory. A detector distance of 5.0 m was selected, which corresponds to a usable K range of $0.03\text{--}0.1 \text{ \AA}^{-1}$; $K = 4\pi\sin\Theta/\lambda$, in which λ is the neutron wavelength (4.75 \AA) and Θ is the half-scattering angle. The wavelength resolution ($\Delta\lambda/\lambda$) is 6%.

The samples were contained in a round quartz cell with a volume of 0.30 ml and a path length of 1.0 mm. The neutron flux passing through the 2.8-cm² sample cell was approximately 10^5 neutrons per sec and each sample was measured for 3 hr.

To prepare the samples for the experiment, two stock solutions of nucleosome core particles, one in H_2O buffer and one in 98% $^2\text{H}_2\text{O}$ buffer, were adjusted to a concentration of 9.0 mg/ml. Appropriate amounts of these stock solutions were mixed to produce 0.30-ml samples at 98%, 73.5%, 24.5%, and 0% $^2\text{H}_2\text{O}$ buffer. The buffer used throughout the experiment was $0.3\times$ TBE (0.0225 M Tris/0.6 mM EDTA/0.0267 M borate, pH 8.3). After the scattering data were collected for each nucleosome sample, 12 μl of HMG 14 stock solution at 35.0 mg/ml in 98% $^2\text{H}_2\text{O}$ buffer was added to the sample already in the quartz cell. (The nucleosome-HMG 14 complex forms immediately and spontaneously in $0.3\times$ TBE.) The proper input level of HMG 14 was previously determined by titrating aliquots of the nucleosome core particle stock solution with the HMG 14 stock solution and analyzing the resulting complex on 5% polyacrylamide particle gels run in $0.3\times$ TBE buffer (Fig. 1). In addition to the samples, appropriate $^2\text{H}_2\text{O}/\text{H}_2\text{O}\text{--}0.3\times$ TBE blanks were collected for proper background correction. Division by scattering from pure H_2O was used to correct for variations in sensitivity across the area of the detector.

RESULTS

The application of neutron scattering to biological systems has been described in detail (15) and in reference to nucleosomes

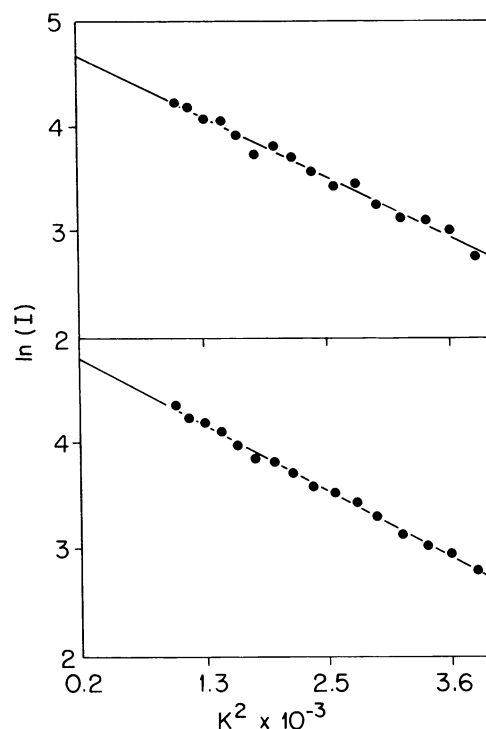


FIG. 2. Typical set of Guinier plots obtained for nucleosomes (Upper) and nucleosome-HMG 14 complex (Lower). Weighted least-squares fits were used to obtain R_g (from the slope) and the intercept. Composition of the solution is $0.3\times$ TBE in $^2\text{H}_2\text{O}$.

(5, 16, 17). A typical pair of Guinier plots of the nucleosome and nucleosome-HMG 14 complex data are shown in Fig. 2. Slopes from the least-squares line of each Guinier plot were used to calculate the R_g directly for each sample:

$$R_g^2 = -3 \times (\text{slope}).$$

The resulting radii are listed in Table 1.

Extrapolation of the least-squares lines on the Guinier plots to zero angle ($K = 0$) gives the zero-angle scattering intensity. A plot of the zero-angle amplitudes ($\sqrt{I(0)}$) vs. solution scattering length density should be linear if there is no great polydispersity in the mean scattering density of the particle (18). The data for nucleosomes and the nucleosome-HMG 14 complex are plotted in Fig. 3. At the point where the scattering amplitude is zero, the mean scattering length density of the particle matches that of the solution. This contrast match point is at 49.4% $^2\text{H}_2\text{O}$ for the nucleosomes and 48.7% $^2\text{H}_2\text{O}$ for the nucleosome-HMG 14 complex, corresponding to solution scattering length densities, ρ_m , of 2.86×10^{10} and $2.82 \times 10^{10} \text{ cm}^{-2}$, respectively.

From the scattering length density of the particle at the match point, the physical volume (anhydrous volume) of the particle, V_f , can be calculated:

$$V_f = \Sigma b_i / \rho_m,$$

where Σb_i is the sum of scattering lengths for the particle taking

Table 1. Summary of data for nucleosomes, nucleosome-HMG 14 complex, and HMG 14

	Measured values of R_g , \AA				Protein match	DNA match	Infinite contrast
	$^2\text{H}_2\text{O}$	75% $^2\text{H}_2\text{O}$	25% $^2\text{H}_2\text{O}$	H_2O			
Nucleosome	38.3 ± 0.4	37.0 ± 0.5	43.8 ± 0.4	41.9 ± 0.3	48.4 ± 0.4	34.5 ± 0.4	40.7 ± 0.4
Nucleosome-HMG 14	40.4 ± 0.3	37.9 ± 0.5	46.3 ± 0.6	43.2 ± 0.4	51.1 ± 0.5	35.4 ± 0.5	42.0 ± 0.5

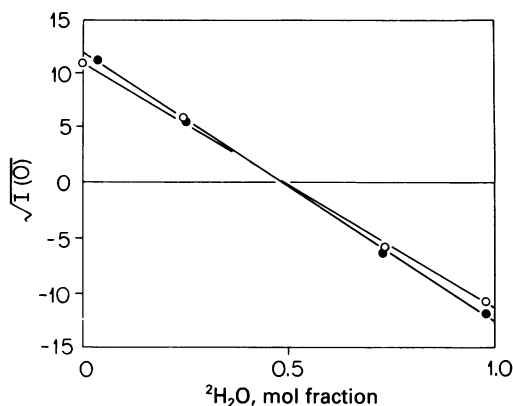


FIG. 3. Plot of $\sqrt{I(O)}$ versus ρ_{sol} , showing nucleosomes (\circ) and nucleosome-HMG 14 complex (\bullet). The intensity units are arbitrary. The match point is 49.4% $^2\text{H}_2\text{O}$ for the nucleosomes and 48.7% $^2\text{H}_2\text{O}$ for the complex.

into consideration hydrogen-deuterium exchange at the match point. In the calculation of $\sum b_i$ for the particles, it was assumed that all 2,674 labile protons in the nucleosome were exchangeable with the exception of 40% of the amide groups (see ref. 17), leaving 2,282 exchangeable protons. All labile protons in the HMG 14, calculated approximately from the calf thymus HMG 14 sequence (19), were assumed to exchange because HMG 14 is in an extended structure (20) and is at equilibrium in the appropriate $\text{H}_2\text{O}/^2\text{H}_2\text{O}$ mixtures before it binds to the nucleosome.

The calculated V_f for the nucleosome is 220.9 nm^3 , which agrees favorably with the recent literature (16). V_f for the nucleosome-HMG 14 complex is calculated to be 244.6 nm^3 , approximately 24 nm^3 larger than the core particle (Table 2). Thus, each of the two HMG 14 molecules may be assumed to have a volume of approximately 12 nm^3 . This is in close agreement with a neutron scattering determination for calf thymus HMG 17 (20), 11.4 nm^3 , and is slightly less than our estimate based on the volumes and relative molecular weights of the more globular histone proteins, 13.6 nm^3 .

The radius of gyration of an object with internal variation of scattering density, as measured by neutron scattering, is a function of the particle's scattering density distribution and the scattering density of the surrounding medium. Stuhrmann (21) has demonstrated that, for an inhomogeneous but essentially centrosymmetric particle, R_g will vary as:

$$R_g^2 = R_f^2 + \alpha/\bar{\rho},$$

where $\bar{\rho}$ is the difference between the mean scattering density of the particle (taking into account exchange of protons) and the surrounding medium and R_f is the radius of gyration of the particle at infinite contrast ($\bar{\rho} = \infty$). A plot of R_g^2 versus $1/\bar{\rho}$ for the nucleosome and the nucleosome-HMG 14 complex is shown in Fig. 4. The mean scattering densities, ρ_{mean} , for the nucleosome and nucleosome-HMG 14 complex particles have been calculated from the relationships:

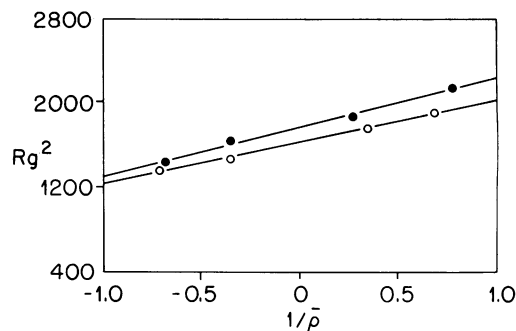


FIG. 4. Plot of R_g^2 versus $1/\bar{\rho}$. \circ , Nucleosomes; \bullet , nucleosome-HMG 14 complex; $\bar{\rho} = \rho_{\text{mean}} - \rho_{\text{sol}}$ for the particle (taking into account proton exchange).

$$\rho_{\text{mean}} = \sum b_i/V_f \text{ and } \bar{\rho} = \rho_{\text{mean}} - \rho_{\text{sol}},$$

where ρ_{sol} is the solution scattering length density.

The significance of the slope of the nucleosome or nucleosome-HMG 14 complex line, as pointed out in the literature (5, 16, 17), is that regions of the particle with different densities have different radii of gyration. More specifically, when DNA dominates the scattering, the radius is considerably larger than when protein dominates. At the protein match point (40% $^2\text{H}_2\text{O}$, $1/\bar{\rho} = 1.8$) R_g for the nucleosome is $48.4 \pm 0.4 \text{ \AA}$, and at the DNA match point (65% $^2\text{H}_2\text{O}$, $1/\bar{\rho} = -1.1$) R_g is $34.5 \pm 0.4 \text{ \AA}$. The measured value of the slope, α , for the nucleosome is $398 \pm 18 \times 10^{-4}$. These values agree favorably with recent literature values (16) in which nucleosome core particles with a DNA length of 146 ± 3 nucleotide pairs were used.

The line for the nucleosome-HMG 14 complex (upper line in Fig. 4) shows behavior similar to that of the nucleosome. The complex is slightly larger and the slope of the line is somewhat steeper, indicating an increase in R_g for both the protein component (which now includes two bound HMG 14 molecules) and the DNA component. The increase in R_g for the DNA component is larger than the increase for the protein component; the slope of the line is $468 \pm 21 \times 10^{-4}$. R_g for the nucleosome-HMG 14 complex at the DNA match point is $35.4 \pm 0.5 \text{ \AA}$, an increase of about 0.9 \AA over that for the nucleosome. (This increase may be entirely the result of adding additional protein to the particle in the form of two HMG 14 molecules.) R_g at the protein match point is $51.1 \pm 0.5 \text{ \AA}$. This is 2.7 \AA larger than the corresponding R_g for the nucleosome, suggesting an alteration of the conformation of the DNA as a result of HMG 14 binding. It should be noted, based on the estimated errors determined from the least-squares fit, that the difference in protein R_g is not statistically significant. The difference in DNA R_g , however, is significant.

At the y intercept of the R_g^2 versus $1/\bar{\rho}$ plot ($\bar{\rho} = \infty$), the contrast between the particles and surrounding solution is infinite. In this situation, internal variations in scattering density are not significant, and R_g represents the radius of gyration of the shape or surface of an essentially homogeneous particle. The radius of gyration at infinite contrast, R_f , is $40.7 \pm 0.4 \text{ \AA}$ for the

Table 2. Calculated values

Variable	Nucleosome	Nucleosome -HMG 14 complex	HMG 14
α , gradient of R_g^2 versus $1/\bar{\rho}$ plot at origin	$398 \pm 18 \times 10^{-4}$	$468 \pm 21 \times 10^{-4}$	—
V_f , dry particle volume, nm^3	220.9	244.6	11.85
V_c , apparent particle volume, nm^3	187.2	208.1	10.45
C_m , contrast match point, % $^2\text{H}_2\text{O}$	49.4	48.7	41.2

nucleosome and $42.0 \pm 0.5 \text{ \AA}$ for the nucleosome–HMG 14 complex.

DISCUSSION

In this study we concentrated on determination and interpretation of the R_g of the nucleosome DNA shell and of the protein core, in the presence or absence of bound HMG 14 (i.e., two HMG 14 per core mononucleosome). The principal findings of this study are: (a) R_g for DNA increased 2.7 \AA in the nucleosome–HMG 14 complex, compared with the nucleosome; (b) R_g for protein increased 0.9 \AA when two HMG 14 were bound.

Interpretation of the structural consequences of these R_g measurements depends upon the choice of the type of perturbations induced in the nucleosomes. Fig. 5 shows some possible perturbations of the core nucleosomal DNA superstructure, starting with the current model (3, 5) of 146-base-pair DNA coiled into a left-handed superhelix of 1.75 turns (pitch, $\approx 30 \text{ \AA}$; overall diameter, $\approx 110 \text{ \AA}$). Two classes of DNA perturbations are considered: (a) uniform distortions of the DNA superhelix due to changes of pitch or radius of curvature; and (b) localized distortions of the DNA due to “hinges” or “bulges”. Fig. 5 presents a summary of the magnitude of DNA perturbation re-

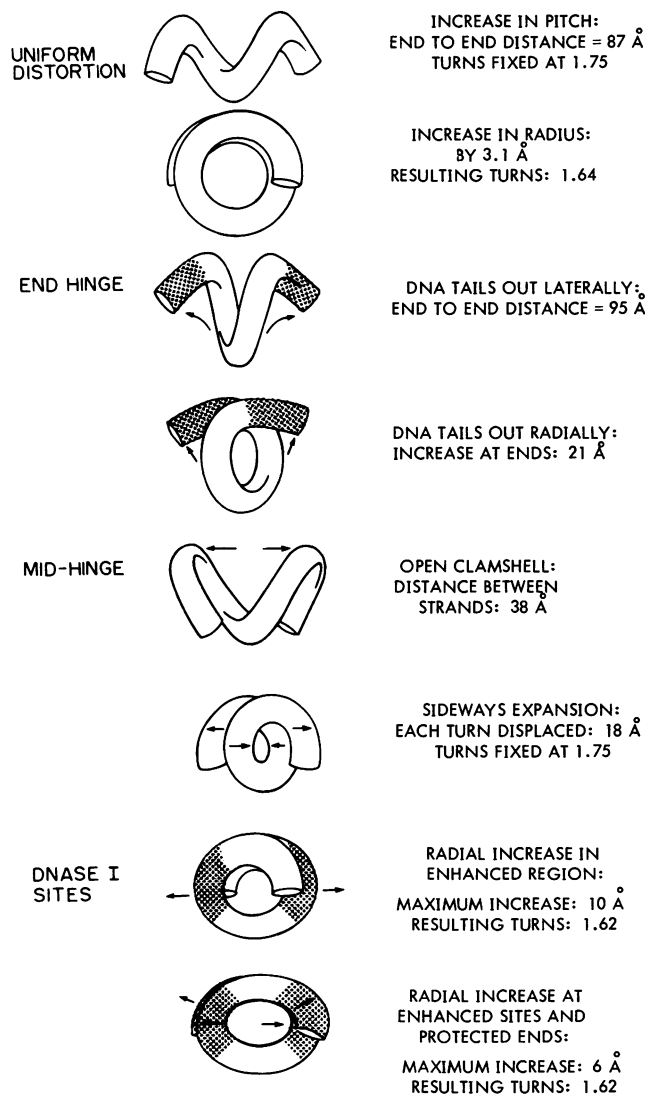


FIG. 5. Some models of DNA perturbations and the magnitudes required to be consistent with the measured DNA R_g of the nucleosome–HMG 14 complex.

quired to be consistent with the measured DNA R_g in the nucleosome–HMG 14 complex.

The small measured increase in the protein R_g when two HMG 14 molecules are bound per nucleosome constitutes an additional constraint upon the range of acceptable models of the mode of DNA distortion. The change we measured in the protein R_g is not consistent with an overall unfolding or opening of the protein core. Our data suggest that the protein core remains relatively unchanged by the binding of HMG 14 and actually may be in a slightly more compact conformation.

Assuming that the basic NH_2 -terminal half of HMG 14 interacts with the nucleosomal DNA tails at 10–20 base pairs from each DNA 5' end (11), we calculated the expected protein R_g for each of the models of DNA perturbation shown in Fig. 5. For each of these cases we considered the following possibilities for the disposition of the rest of the HMG peptide chain with respect to the path of nucleosomal DNA: (a) the COOH-terminal half of the peptide chain remains coaxial with the DNA, (b) the remainder of each HMG binds inside the R_g of the protein at the surface of the globular core, and (c) the remainder of each HMG 14 interacts with the “free” NH_2 -terminal tails of H2A and H2B (5, 22) and both together occupy a region inside the R_g of the protein at the surface of the globular core.

For all the models of DNA perturbation considered in Fig. 5, coaxial binding of the entire HMG peptide chain to the DNA helix resulted in too great a predicted protein R_g . Furthermore, various models of DNA perturbation never predicted realistic protein R_g with any of the present assumptions. The models involving end-hinges and the increase in superhelix pitch were too extended to be compatible with the observed increase in protein R_g of only 0.9 \AA , assuming that some histone and (or) HMG protein was associated with the ends of the DNA. This assumption is based on experiments that show protection of the DNA ends from susceptibility to DNase I upon binding of HMG 14 (8, 11). The sideways expansion and open clam shell models require significant changes in protein conformation leading to changes in protein R_g that are contrary to our experimental results. For some models the results were acceptable with assumption b. For these models, calculation of the protein R_g generally predicted more realistic values when it was assumed that the histone tails interacting with the COOH-terminal portion of the HMG 14 peptide chain were also displaced toward the globular protein core. This modeling result suggests that the octamer in fact may be in a slightly more compact conformation when HMG 14 is bound.

The acceptable models include some of the more subtle perturbations in the DNA superhelix. One such perturbation consists of an uplifting of the DNA at the DNase I sites, amounting to a maximal radial displacement of 10 \AA (fitting a Gaussian form with a full width at half maximum of 20 base pairs). We refer to this as the “one-bulge” model. A second subtle model, the “two-bulge” case, includes uplifting of the DNA superhelix at the ends as well as at the DNase I sites. In this model the maximal displacement of the DNA superhelix is 6 \AA ; the full width at half maximum of the bulge remains at 20 base pairs. Based on modeling calculations, a uniform decrease in curvature (increase in the radius of the entire DNA) also seems acceptable. Further discrimination between the possible models of DNA and protein shape must await analysis of higher-angle neutron scattering data.

It is apparent that HMG 14 binding to bulk nucleosomes causes subtle changes in the conformation of the DNA superhelix. It is also clear that binding HMG 14 to such nucleosomes does not produce changes consistent with any major rearrangement of the histone core. One principal feature of the acceptable models is that they all show a radial increase of the DNA and

a slight unwinding of the DNA superhelix to about 1.65 turns. Another interesting feature of the acceptable models is that generally better agreement with the protein R_g is obtained if one assumes a movement of histone tails inward from presumed contacts with the DNA. If extrapolation to active nucleosomes is possible, these results suggest that the DNase I sensitivity of active nucleosomes may be the result of a slight unwinding of the DNA and, just as importantly, a movement by portions of the histone octamer inward to form a more compact protein structure.

There is evidence (23) that perhaps all active nucleosomes contain undermethylated DNA and an altered histone octamer conformation. In addition, a subpopulation of these nucleosomes contain hyperacetylated histones and topoisomerase I (23). Active nucleosomes show enhanced binding affinity for HMG 14 and HMG 17 compared to bulk nucleosomes (23). We do not know how closely the conformational changes observed in this study resemble the effect of HMG 14 and HMG 17 on active nucleosomes. There is some evidence, however, that would imply similarity. For example, studies of the adult chicken erythrocyte β -globin gene have shown that, in the presence of excess HMG 14 (HMG 17), this gene remains as condensed as bulk chromatin (24), suggesting that the HMG 14 (HMG 17) is not promoting any overall nucleosome unfolding and chromatin unwinding. In order to understand the unique properties of active gene regions it will be necessary to study HMG 14 and HMG 17 binding in the context of the other factors identified with active nucleosomes.

We acknowledge the strong support provided by Dr. Alexander Zucker (Associate Director of Physical Sciences, Oak Ridge National Laboratory). We also thank W. C. Koehler, R. H. Child, and G. D. Wignall (National Center for Small-Angle Scattering Research), L. B. Maddox (Computer Sciences Division, Oak Ridge), G. Zaccai (Institut Max Von Laue-Paul Langevin, Grenoble, France) for helpful discussions, B. E. Hingerty (Biology Division, Oak Ridge) for some of the model calculations, W. E. Thiessen and R. Triolo (Chemistry Division, Oak Ridge) for their efforts during the initial phase of this work, and E. Wilkinson-Singley for valuable criticisms of the manuscript. This research was sponsored by the Division of Materials Sciences, the Office of Health and Environmental Research, U.S. Department of Energy, under Contract W-7405-eng-26 with the Union Carbide Corporation, and National Institutes of Health Research Grants GM 19334 to D.E.O. and GM 29818 to G.J.B.; E.C.U. and J.K.W.M. were Post-doctoral Investigators supported by Subcontract 3322 from the Biology Division, Oak Ridge National Laboratory, to the University of Ten-

nessee. R.M.R. was supported by a research assistanceship granted by the University of Tennessee.

1. Felsenfeld, G. (1978) *Nature (London)* **271**, 115–122.
2. Igo-Kemenes, T., Hörz, W. & Zachau, H. G. (1982) *Annu. Rev. Biochem.* **51**, 89–121.
3. Finch, J. T., Lutter, L. C., Rhodes, D., Brown, R. S., Rushton, B., Levitt, M. & Klug, A. (1977) *Nature (London)* **269**, 29–36.
4. Klug, A., Rhodes, D., Smith, J., Finch, J. T. & Thomas, J. O. (1980) *Nature (London)* **287**, 509–516.
5. Braddock, G. W., Baldwin, J. P. & Bradbury, E. M. (1981) *Bio-polymers* **20**, 327–343.
6. Bentley, G. A., Finch, J. T. & Lewit-Bentley, A. (1981) *J. Mol. Biol.* **145**, 771–784.
7. Albanese, I. & Weintraub, H. (1980) *Nucleic Acids Res.* **8**, 2787–2805.
8. Sandeen, G., Wood, W. I. & Felsenfeld, G. (1980) *Nucleic Acids Res.* **8**, 3757–3778.
9. Weisbrod, S. & Weintraub, H. (1979) *Proc. Natl. Acad. Sci. USA* **76**, 630–634.
10. Weisbrod, S., Groudine, M. & Weintraub, H. (1980) *Cell* **19**, 289–301.
11. Mardian, J. K. W., Paton, A. E., Bunick, G. J. & Olins, D. E. (1980) *Science* **209**, 1523–1536.
12. Lutter, L. C. (1978) *J. Mol. Biol.* **124**, 391–420.
13. Goodwin, G. H., Nicolas, R. H. & Johns, E. W. (1975) *Biochim. Biophys. Acta* **405**, 280–291.
14. Rabbani, A., Goodwin, G. H. & Johns, E. W. (1978) *Biochem. Biophys. Res. Commun.* **81**, 351–358.
15. Zaccai, G. (1978) in *Topics in Current Physics: Neutron Diffraction*, ed. Dachs, H. (Springer-Verlag, Berlin), pp. 243–270.
16. Bradbury, E. M., Baldwin, J. P., Suau, P., Hjelm, R. P., Braddock, G. W., Kneale, G. G. & Carpenter, B. G. (1981) in *Bio-molecular Structure, Conformation, Function, and Evolution, Vol. 1, Diffraction and Related Studies*, eds. Srinivasan, R., Subramanian, E. & Yathinda, W. (Pergamon, New York), pp. 405–413.
17. Hjelm, R. P., Kneale, G. G., Suau, P., Baldwin, J. P. & Bradbury, E. M. (1977) *Cell* **10**, 139–151.
18. Stuhmann, H. B. & Duee, E. D. (1975) *J. Appl. Crystallogr.* **8**, 338–342.
19. Walker, J. M., Goodwin, G. H. & Johns, E. W. (1979) *FEBS Lett.* **100**, 394–398.
20. Abercrombie, B. D., Kneale, G. G., Crane-Robinson, C., Bradbury, E. M., Goodwin, G. H., Walker, J. M. & Johns, E. W. (1978) *Eur. J. Biochem.* **84**, 173–177.
21. Stuhmann, H. B. (1974) *J. Appl. Crystallogr.* **7**, 173–178.
22. Cary, P., Moss, T. & Bradbury, E. M. (1978) *Eur. J. Biochem.* **89**, 475–482.
23. Weisbrod, S. T. (1982) *Nucleic Acids Res.* **10**, 2017–2042.
24. McGehee, J. D., Rau, D. C. & Felsenfeld, G. (1982) *Nucleic Acids Res.* **10**, 2007–2016.